Supplementary Information

Synthesis of $Co_3O_4/SnO_2@MnO_2$ Core-Shell Nanostructures for High-Performance Supercapacitors

Ming Huang[a], Xiao Li Zhao[a], Fei Li[a], Wei Li[b,*], Bo Zhang[c], Yu Xin Zhang[a,d,*]

[a] College of Material Science and Engineering, Chongqing University, Chongqing 400044, P.R. China

[b] Department of Chemistry and Laboratory of Advanced Materials, Fudan University, Shanghai 200433, People's Republic of China

[c] Department of Cardiology, Xinqiao Hospital, Third Military Medical University, Chongqing 400037, P.R. China

[d] National Key Laboratory of Fundamental Science of Micro/Nano-Devices and System Technology, Chongqing University, Chongqing 400044, P.R. China

[*]E-mail: zhangyuxin@cqu.edu.cn; li_w10@fudan.edu.cn

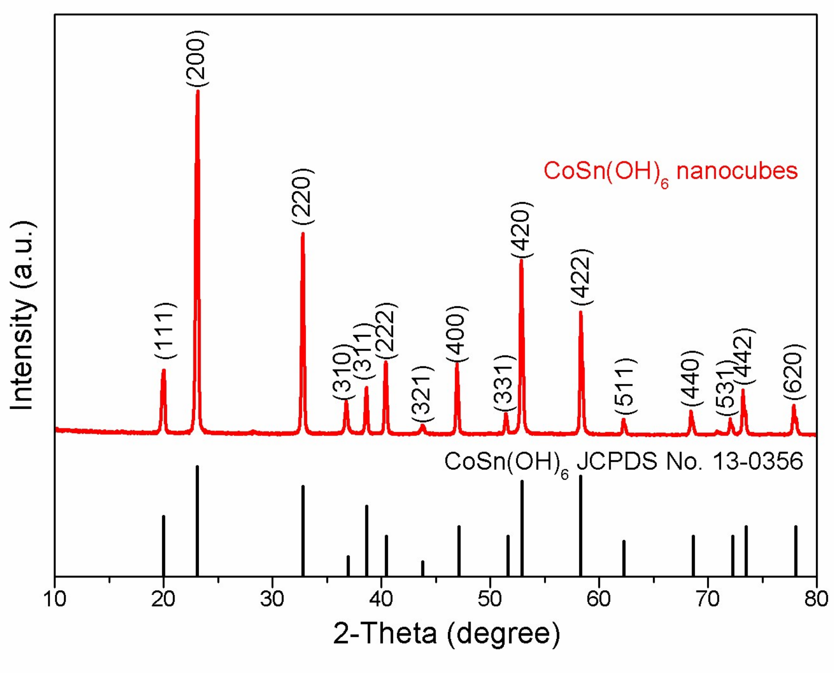

Fig. S1. XRD pattern of $CoSn(OH)_6$ nanocubes

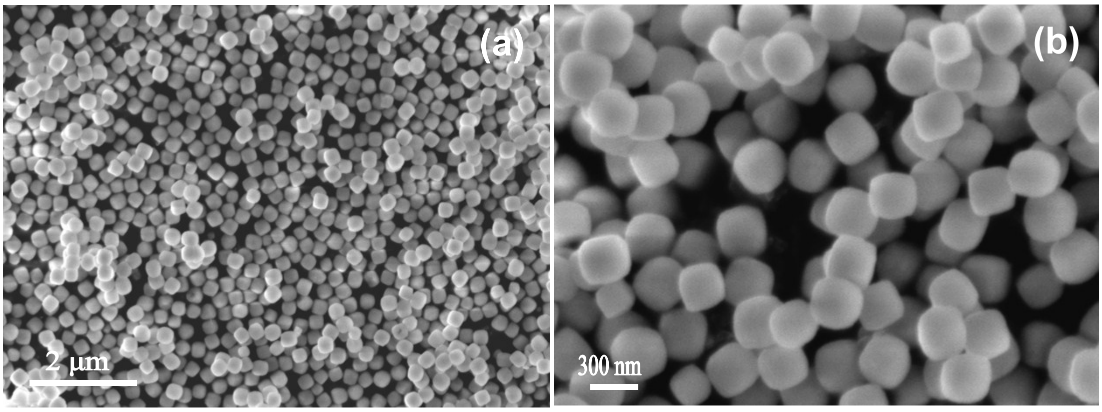

Fig. S2. SEM images of the as-prepared $CoSn(OH)_6$ nanocubes.

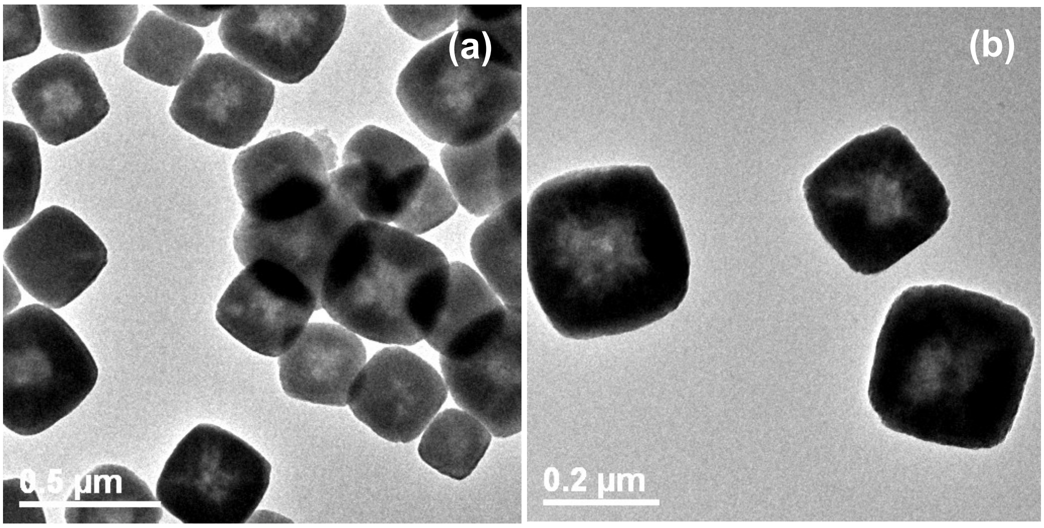

Fig. S3. TEM images of $CoSn(OH)_6$ nanoboxes obtained by the NaOH etching process.

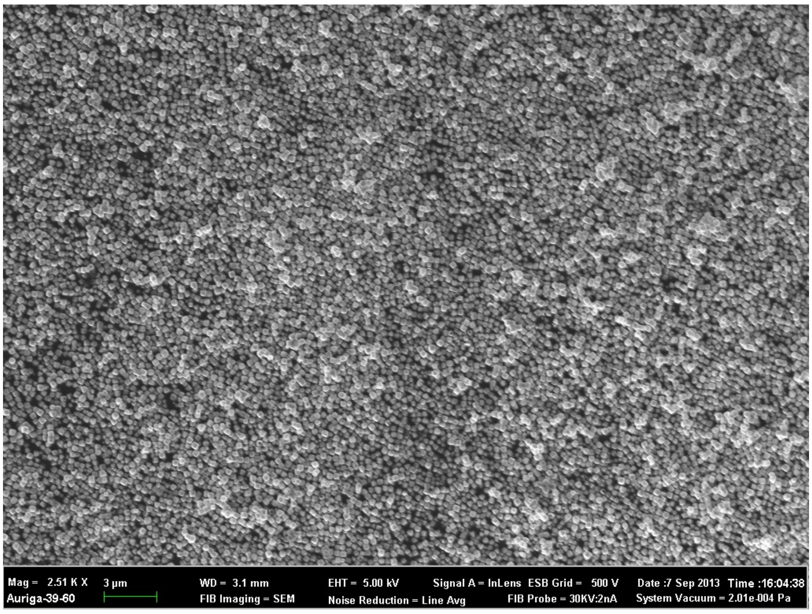

Fig. S4. Large-area SEM image of Co_3O_4/SnO_2 nanoboxes.

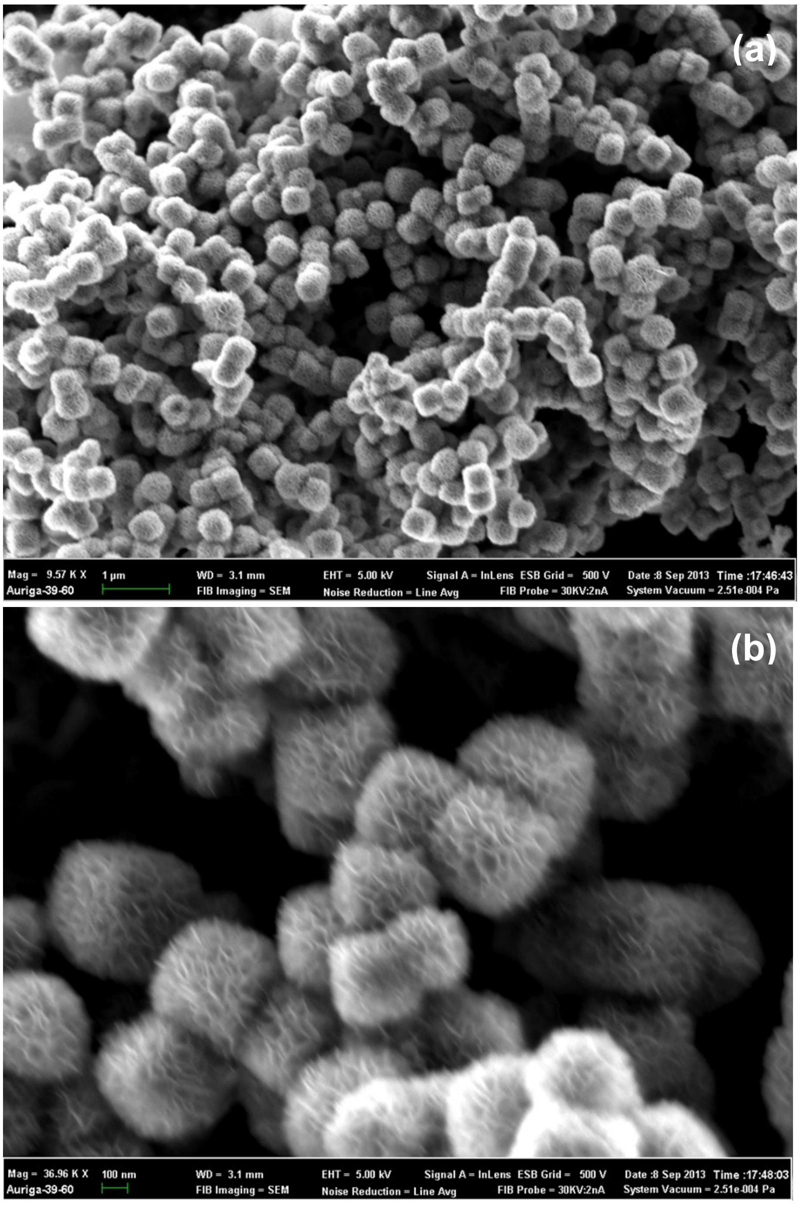

Fig. S5. SEM images of $Co_3O_4/SnO_2@MnO_2$ core-shell nanostructures with different magnifications.

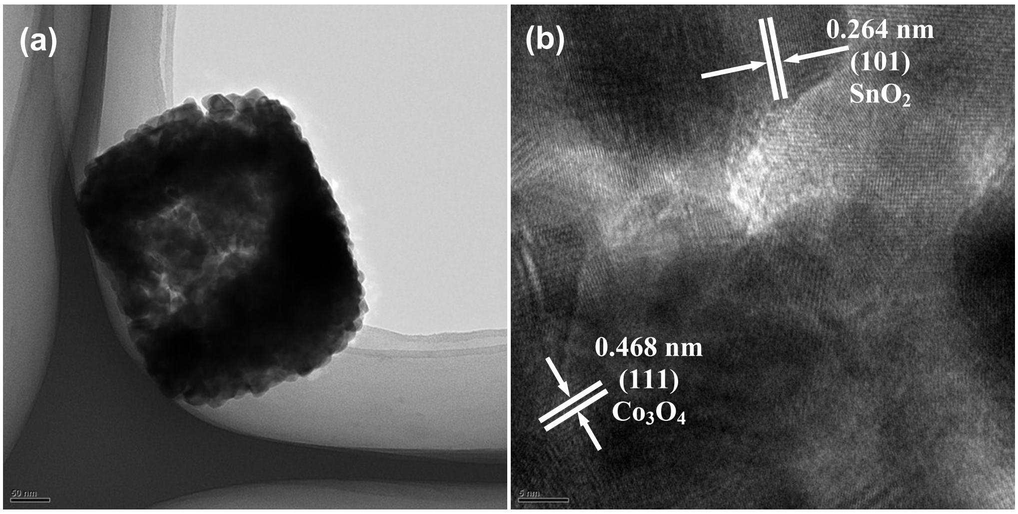

Fig. S6. Low-magnification TEM image (a) and HRTEM image (b) of the Co_3O_4/SnO_2 nanobox.

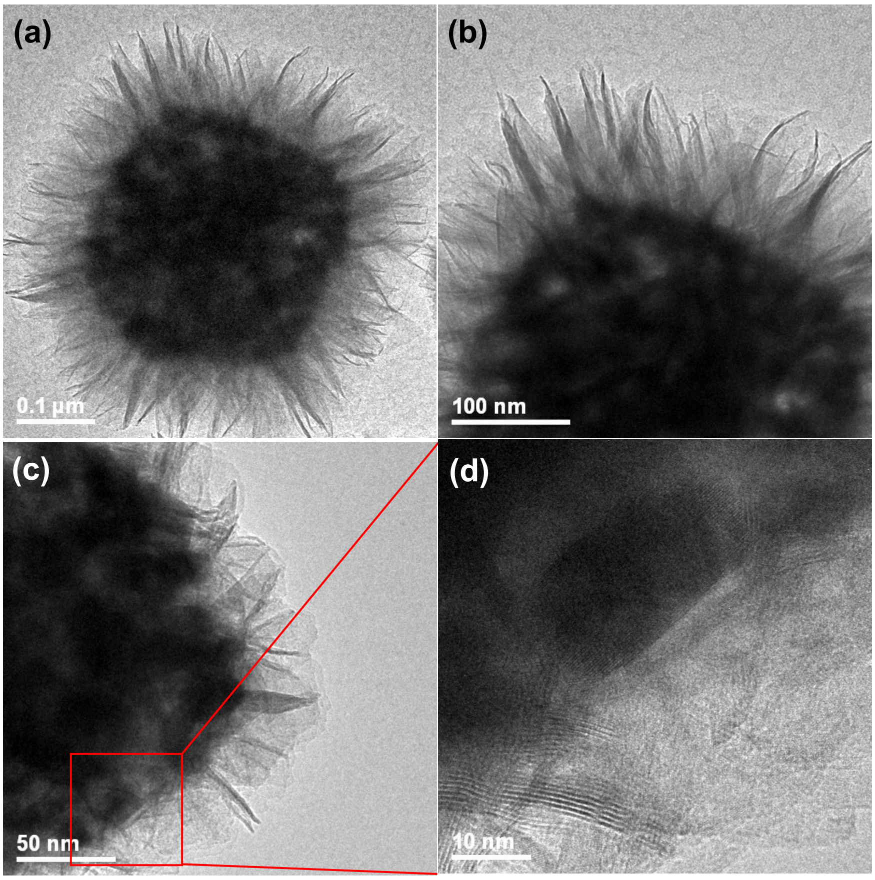

Fig. S7. (a-c) TEM images of the $Co_3O_4/SnO_2@MnO_2$ core-shell nanostructures at different magnifications; (d) HRTEM image of the boxed region in (c).

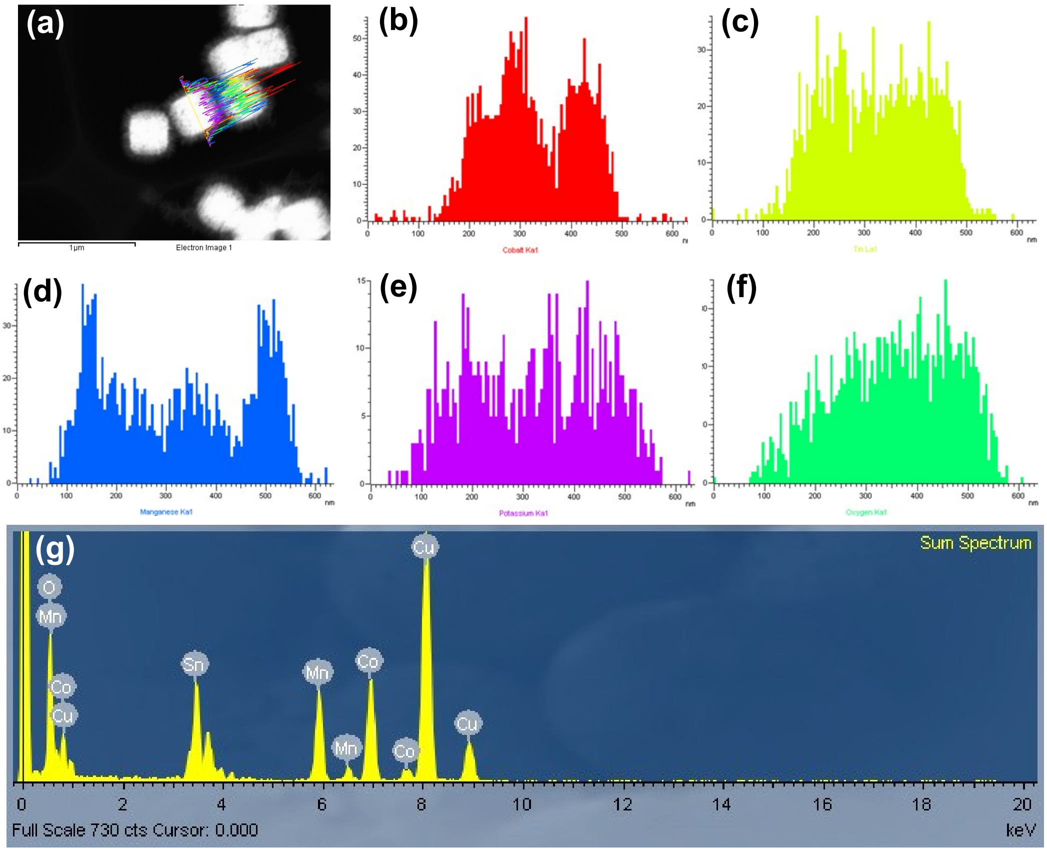

Fig. S8. (a) STEM image of $Co_3O_4/SnO_2@MnO_2$ core-shell nanostructures; (b-g) EDS results of the line scan for the indicated line in the nanocomposite, demonstrating the MnO_2 nanosheets layers decorated on the surface of Co_3O_4/SnO_2 nanobox.

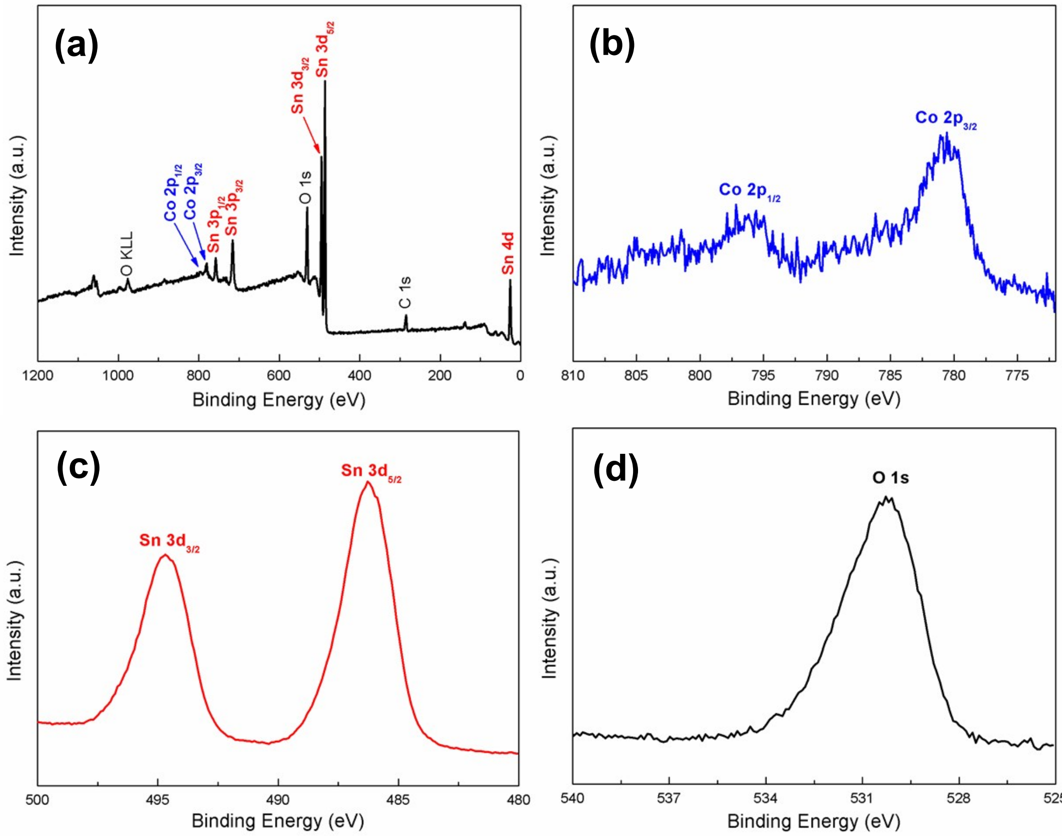

Fig. S9. XPS spectra of Co_3O_4/SnO_2 nanoboxes: (a) XPS survey scan; (b) Co 2p spectrum; (c) Sn 3d spectrum; (d) O 1s spectrum.

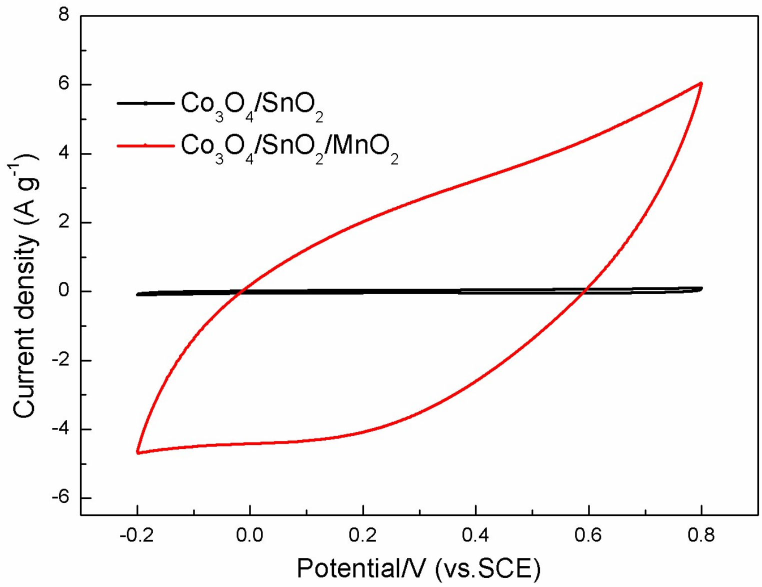

Fig. S10. CV curves of Co_3O_4/SnO_2 and Co_3O_4/SnO_2@MnO_2 core-shell nanostructure electrode at a scan rate of 50 mV s^{-1}.

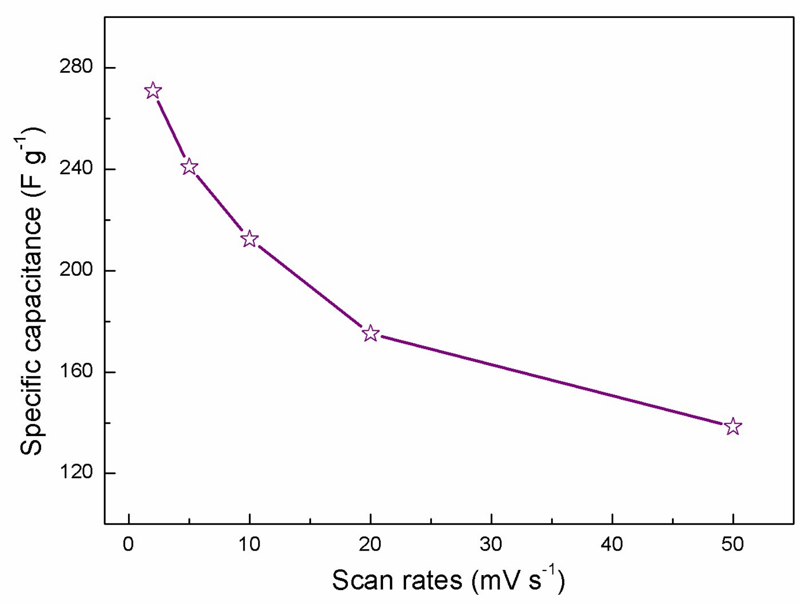

Fig. S11. The specific capacitances of the $Co_3O_4/SnO_2@MnO_2$ electrode measured at different scan rates.

Discussion: The specific capacitance of the electrode can be calculated from the CV curves according to the following equation:

$$C_m = \frac{i}{mv}$$

where m is the mass of electro-active material, v is the potential sweep rate, and i is the current response defined by

$$i = \int_{V_a}^{V_c} i(V)dV/(V_c - V_a)$$

V_a and V_c represent the lowest and highest voltages, respectively.

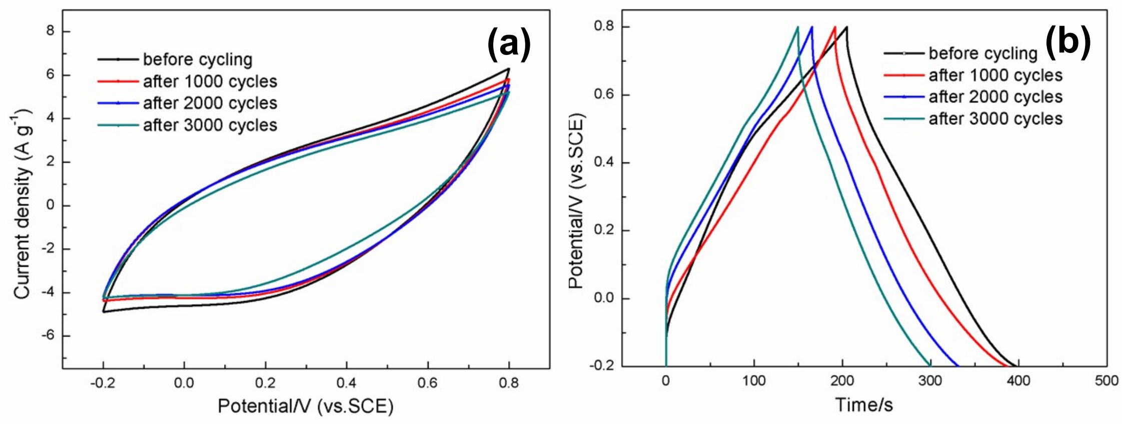

Fig. S12. (a) CV curves of $Co_3O_4/SnO_2@MnO_2$ core-shell nanostructure electrode during charge/discharge cycles at a scan rate of 50 mV s^{-1}; (b) the corresponding charge/discharge curves of the electrode at a current density of 1 A g^{-1}.

Table. S1. Comparison of mass loading and the electrochemical properties of MnO_2-based composite electrodes. All values are obtained in three-electrode system.

Samples	Electrode mass (mg cm^{-2})	*Cs* (Fg^{-1})	Test condition	References
$Co_3O_4/SnO_2@MnO_2$	3.8	225	0.5 A g^{-1}	Current work
RGO/MnO_2	2	260	0.3 A g^{-1}	1
CNTA/Au/Mn_3O_4	5.46	143	2 mV s^{-1}	2
CNFs/MnO_2	0.68	419	1 A g^{-1}	3
CF-CNTA/MnO_2	4.09	326	2 mV s^{-1}	4
CNTs/MnO_2	4.85	144	0.5 A g^{-1}	5
MWNT/MnO_2	\	208	5 mV s^{-1}	6
CNTs/ITO/MnO_2	\	290	10 mV s^{-1}	7
ATO/MnO_2	\	187	0.25 A g^{-1}	8
Carbon spheres/MnO_2	5	190	0.1 A g^{-1}	9
CNT/PEDOT-PSS/MnO_2	1.5	200	3.3 A g^{-1}	10
CNT textile/MnO_2	0.8	185	5 mV s^{-1}	11
CNTs/Pt-Si/MnO_2	0.1	471	10 mV s^{-1}	12
CuO/MnO_2	2	167	0.3 A g^{-1}	13
NiO/MnO_2	10	453	2 A g^{-1}	14
Diatomite/MnO_2	2	203	0.5 A g^{-1}	15
Graphene/NiO-MnO_2	\	242	0.2 mV s^{-1}	16
Bi_2O_3/MnO_2	\	139	0.2 A g^{-1}	17
$Co_3O_4@Pt@MnO_2$	0.3	539	1 A g^{-1}	18
CNT arrays/MnO_2	6.7	199	1 A g^{-1}	19

References

1. J. Zhang and X. S. Zhao, *Carbon*, 2013, **52**, 1-9.
2. X. Cui, F. Hu, W. Wei and W. Chen, *Carbon*, 2011, **49**, 1225-1234.
3. J.-G. Wang, Y. Yang, Z.-H. Huang and F. Kang, *Electrochim. Acta*, 2011, **56**, 9240-9247.
4. P. Lv, P. Zhang, Y. Feng, Y. Li and W. Feng, *Electrochim. Acta*, 2012, **78**, 515-523.
5. X. Jin, W. Zhou, S. Zhang and G. Z. Chen, *Small*, 2007, **3**, 1513-1517.
6. H.-Y. Chu, Q.-Y. Lai, L. Wang, J.-F. Lu and Y. Zhao, *Ionics*, 2010, **16**, 233-238.
7. S. W. Lee, J. Kim, S. Chen, P. T. Hammond and Y. Shao-Horn, *ACS Nano*, 2010, **4**, 3889-3896.
8. Z. Zhang, C. Ma, L. He, M. Huang, L. Yu and Y. Zhang, *Ceram. Int.*, 2014, **40**, 10309-10315.
9. Z. Lei, J. Zhang and X. Zhao, *J. Mater. Chem.*, 2012, **22**, 153-160.
10. Y. Hou, Y. Cheng, T. Hobson and J. Liu, *Nano Lett.*, 2010, **10**, 2727-2733.
11. L. Hu, W. Chen, X. Xie, N. Liu, Y. Yang, H. Wu, Y. Yao, M. Pasta, H. N. Alshareef and Y. Cui, *ACS Nano*, 2011, **5**, 8904-8913.
12. K.-W. Nam, C.-W. Lee, X.-Q. Yang, B. W. Cho, W.-S. Yoon and K.-B. Kim, *J. Power Sources*, 2009, **188**, 323-331.
13. Y. X. Zhang, F. Li and M. Huang, *Mater. Lett.*, 2013, **112**, 203-206.
14. E.-H. Liu, W. Li, J. Li, X.-Y. Meng, R. Ding and S.-T. Tan, *Mater. Res. Bull.*, 2009, **44**, 1122-

1126.
15. Y. X. Zhang, M. Huang, F. Li, X. L. Wang and Z. Q. Wen, *J. Power Sources*, 2014, **246**, 449-456.
16. S.-G. Hwang, J.-E. Hong, G.-O. Kim, H. M. Jeong and K.-S. Ryu, *ECS Solid State Lett.*, 2013, **2**, M8-M11.
17. J. Ma, S. Zhu, Q. Shan, S. Liu, Y. Zhang, F. Dong and H. Liu, *Electrochim. Acta*, 2015, **168**, 97-103.
18. H. Xia, D. Zhu, Z. Luo, Y. Yu, X. Shi, G. Yuan and J. Xie, *Sci. Rep.*, 2013, **3**, 2978.
19. H. Zhang, G. Cao, Z. Wang, Y. Yang, Z. Shi and Z. Gu, *Nano lett.*, 2008, **8**, 2664-2668.

Table S2. Equivalent circuit parameters fitted from Nyquist plots for $Co_3O_4/SnO_2@MnO_2$ core-shell nanostructure electrodes after different charge/discharge cycles.

Samples	*Rs* (ohm cm^2)	CPE$_1$;Y_0 (Ss^{-n} cm^{-2})	n	*Rct* (ohm cm^2)	*Zw; Y$_0$* (Ss$^{-0.5}$ cm^{-2})	C_L (F cm^{-2})
Before cycling	3.136	7.453×10^{-3}	0.81	9.729	0.1338	0.228
After 1000 cycles	3.169	1.464×10^{-3}	0.78	12.96	0.1103	0.243
After 3000 cycles	3.331	2.071×10^{-3}	0.79	13.37	0.0696	0.198